LINE SHAPE ANALYSIS OF LINEAR X RAY MAGNETIC SCATTERING COPT THIN FILMS

E.V.R.CHAN

University of Washington,Box 351560
Seattle, Washington, 98195-2420, United States.

evr@u.washington.edu

Data analysis of the CCD files from x ray magnetic resonance scattering linearly polarized in transmission geometry produces information about the radial and azimuthal intensities. In a series of measurements of increasing photon energies trends in data are analyzed.

1. Introduction

Magnetic thin film systems and multilayer systems have been studies very actively because of their magnetic properties and possible application for practical devices, such as magnetic recording media technologies.

2. Experiment

Samples were grown on smooth, low-stress, 160 nm. thick SiNx membranes by magnetron sputtering; they all had 20 nm. thick Pt buffer layers and 3 nm. thick Pt caps. Between the buffer layer and the cap, the samples had 50 repeating units of a 0.4 nm. thick Cobalt layer and a 0.7 nm. thick Pt layer. Experiments used linearly polarized x rays from the Advanced Light Source at Lawrence Berkeley Laboratory (supported by USDOE), the thirteenth harmonic of the beamline 9, undulator gap of 54 mm. near the resonant Cobalt L edge. To achieve transverse coherence, the raw undulator beam was passed through a 35 micron diameter pinhole before being scattered in transmission by the sample. The distance from the sample to the CCD is 118 cm. The resonant magnetic scattering was collected by the Princeton soft x-ray CCD camera 1024 X 1024 pixels in an area one inch by one inch. The intensity of the raw undulator beam was 2 X 10 ** 14 photons/sec., the intensity of the coherent beam was 2 X 10 ** 12 photons/sec., and the intensity of the scattered beam, was 2 X 10 ** 7 photons/sec. Each speckle pattern was measured for 30 to 100 seconds, so the total number of photons in each CCD image 1024 X 1024 pixels is about 10 ** 9. The speckle patterns may be used to reconstruct the magnetic domain structure of the sample[1–3]; this is but one of a general class of the old inverse or phase retrieval problems[4].

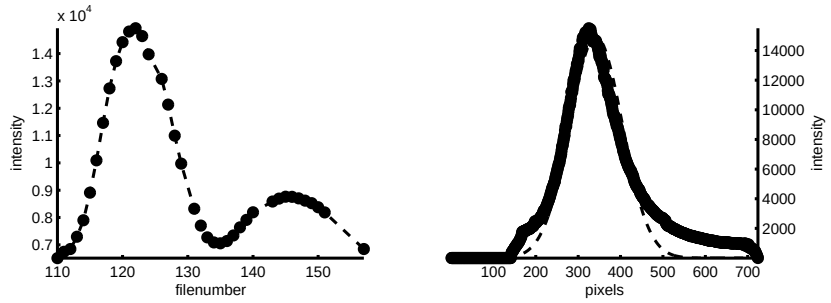

Fig. 1. (left) Average intensity versus filenumber for the series of images. (right) Azimuthally averaged radial intensity of image file 122.

3. Data Analysis

The data appears as a series of CCD image files 726Axxx.SPE (of increasing photon energy) that is read into the data processing computer program. The file numbers can be converted to photon energy since the difference between the two maxima files 122 (photon energy 779.2 eV.) and 145 is 15.8 eV. Figure 1 (left) shows the magnetic resonance has two peaks. Each piece of data has an image file associated and that file has a 1024 X 1024 matrix containing intensity values (if plotted in 3D it has the shape of a centered crown). The Princeton CCD camera file is read into the freely available Matlab data analysis program by the following code fragment:

```
%auto-ignore
fid=fopen('nameOfFile.SPE','r');
header=fread(fid,2050,'uinit16'); %half of 4100 bytes
ImMat=fread(fid,1024*1024,'uint16');
Z=reshape(ImMat,1024,1024);
fclose(fid);Z=double(Z);
[X,Y]=meshgrid(1:1024,1:1024);
mesh(X,Y,Z); %display 3D plot
axis square; axis tight; view(90,90);
print -djpeg99 nameOfFile.jpg %highest resolution saved
%send email  evr@u.washington.edu
```

Figure 1(right) shows the variation of the intensity in file 122 in the radial direction that has been azimuthally averaged (consider slicing through the center out past the edge of the crown). The data analysis calculates the radius of each pixel, places it into appropriate bins and finds the average intensity; since each bin is only one pixel wide the bin number is the radius rounded to integer. The profile was fitted to a gaussian using non-linear Levenberg-Marquardt least squares. The difference between the maximum and minimum calculated values is the height, the distance of the maximum from the origin is called the peak center, and the FWHM (full width at half maximum) is called the width. More about the variation of the height, width

Table 1. Normalized Cross-Correlation

	117	122	133	145
117	1.0	0.8	-0.8	-0.8
122	0.8	1.0	-0.9	-0.9
133	-0.8	-0.9	1.0	0.9
145	-0.8	-0.9	0.9	1.0

and center with filenumber will appear at the end.

4. Results and Discussion

The series of files 726Axxx.SPE are analysed for normalized cross-correlation[5] using 2D matrices of the image files from which the average pixel values have been subtracted. The sum of the product of pixel values from two images divided by the square root of the product of the sum of the pixel values squared of each image (makes it normalized) is gamma (normalized cross-correlation) of the two images. If gamma is 1 they are correlated, if zero uncorrelated and if -1 anti-correlated. The normalized cross-correlation function, gamma, is related to the coherence function[6]. Table 1 shows the values of gamma for four of the files selected as file 117(middle of first peak), file 122 (top of first peak), file 133 (minimum between the two peaks) and file 145 (top of second peak).

The CCD images were processed so as to remove the burns, remove anomalous charge scattering, remove the blocker arm, centered in the image and the central disk darkened to remove the burns in that area also. The bright spots on the image are fixed burns in the CCD camera that cause a few pixels to be unusable; these are the ones that appear very bright. At the end of a series of SPE image files a CCD burns only image was taken and a burns and anomalous charge scattering image was taken. The difference of these two images was used to subract off the anomalous charge scattering pisels from each image file pixels (provided they are above the minimum background value of the image). After the anomalous charge scattering is removed, the burns (or hot spots) are removed. The hot spots are masked off, and after rotating around the middle of the 1024 X 1024 image, new background replaces the hot spots. Next, the circle of maximum intensity is found by having an imaginary turtle going out from beyond the edge of the blocker disc in rays every 1 degree finding maximum intensity. The intensities are sorted, the lowest 20 points out of 360 dropped and a least squares fit of the 340 points is done yielding the circle of maximum intensity. The approximate edges of the blocker arm (about 7 degrees) are located by finding those points on the circle of maximum intensity where the second derivative changes sign. A mask is created, a rotation picks up a patch, and the pixels of the blocker arm are replaced. Missing background is fille in on the edges to make 1024 X 1024. All pixels further out from the center, beyond the circle of maximum intensity were used to find the centroid and then the whole

pattern was relocated to the center of the image matrix.

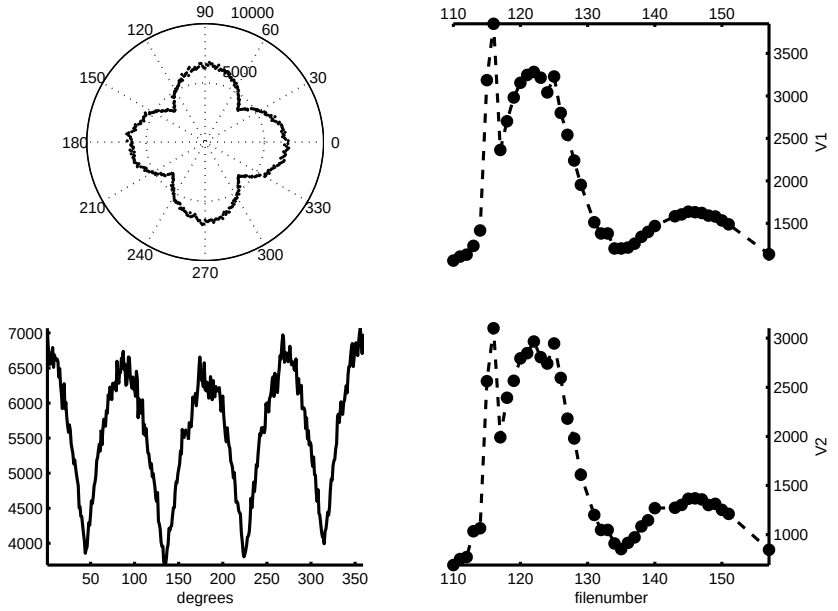

Fig. 2. (upper left)Polar plot of average azimuthal angular intensity looking down the z axis at file 122 (lower left) azimuthal angular intensity of file 122 (upper right) V1 versus filenumber where V1 is the difference between the first maximum azimuthal radially averaged intensity and the lowest minimum (lower right) V2 versus filenumber where V2 is the difference between the second maximum azimuthal radially averaged intensity and the lowest minimum

Due to the use of coherent light from synchrotron radiation, the scattering patterns produced are highly speckled. Each speckle is the sum of light scattered from all the illuminated magnetic domains. So small changes in the microscopic orientation of the magnetic domains can have a large effect on the speckle pattern. The bulk magnetization of Cobalt usually is in the x-y plane but when there are only a few Cobalt atoms in the layer the magnetication becomes perpendicular to the plane of the layers. The observed intensity is related to the charge density, polarization, photon energy, magnetization, atomic scattering factor and scattering geometry; there are terms due to magnetic resonance and electronic structure[7].

The azimuthal variation of intensity is calculated by looking at the angle from the center for each pixel, classifying it as belonging to bins (1 to 360) and finding the average of each bin; this is plotted versus the bin number with each bin being one degree wide. In Fig. 2 the difference between the maxima and the lowest minimum is V1, V2. The azimuthal variation of the intensity is described by an equation for magneto-crystalline anisotropy energy that includes a term proportional to the sine of twice the azimuthal angle squared[8]. The amplitude has real and imaginary

charge and magnetic anomalous scattering factors which are tensors in the general case[9].

The right side of Fig. 2 pretty much follows the shape of average intensity versus file number in Fig. 1(left) and illustrates the variation of the magnetic anisotropy difference (maximum minus lowest minimum) with photon energy(increases with file number). The average of the value of first maximum and second maximum would be a reasonable estimate of the variable. The reason the magnetic anistropy has these variations is because the atomic factor is a tensor[10].

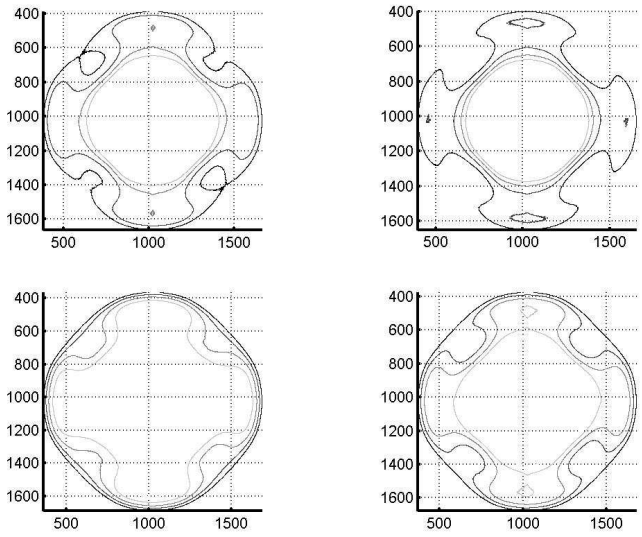

Fig. 3. (upper left)contour plot of autocorrelation file 117 halfway up first peak, (lower left) contour plot of autocorrelation file 133 minimum between peaks, (upper right)contour plot of autocorrelation file 122 tope of first peak, (lower right) contour plot of autocorrelation file 145 top of second peak

The autocorrelation has a maximum at the origin. You could think of it as the convolution of the complex conjugate of f(-x,-y) and f(x,y). If f(x,y) has a Fourier transform F(s,r), then its autocorrelation function has the transform absolute value squared of F(s,r) and has no phase information(Wiener-Khinchin theorem). In the data analysis, the autocorrelation is evaluated by taking the Fourier transform of the reverse complex conjugate of the image and the Fourier transform of the image, then taking the real part of the inverse Fourier transform of the product of these two Fourier transforms. The three dimensional plot of the autocorrelation looks like a mountain with a narrow spike in the middle. The threshholded (25-30%) contours(5)

in the x-y plane of the different files show more variation and different symmetries. Figure 3(upper left) File 117, halfway up the first peak, looks like it has four 2-fold axes. Figure 3(upper right) File 122, at the top of the first peak, may have one 4-fold and two 2-fold axes. Figure 3(lower left) File 133, the minimum between the peaks, appears to have one 4-fold axis and two 2-fold axes. Figure 3(lower right) File 145, top of the second peak, seems to have four 2-fold axes.

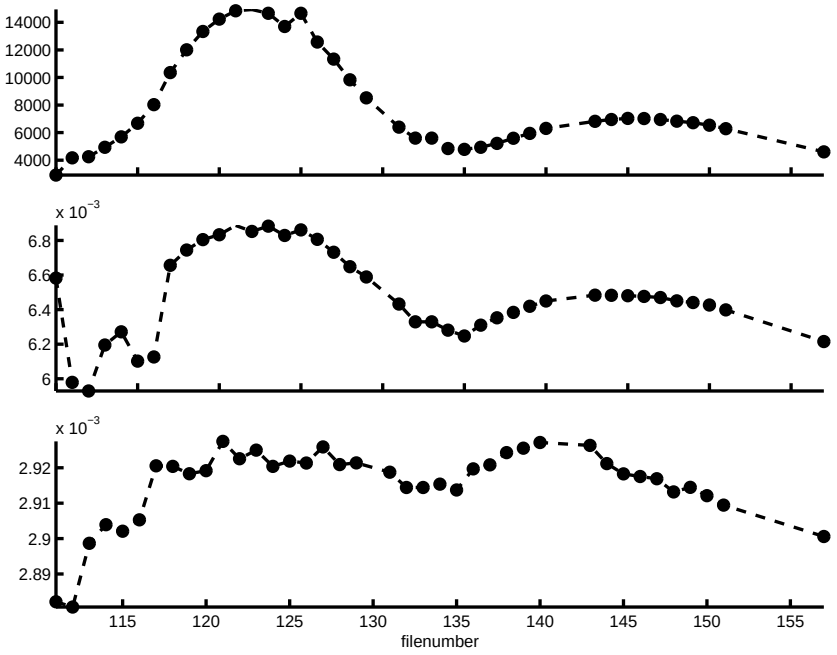

Fig. 4. (top) Peak height from the fitted gaussian versus filenumber (middle) Inverse of the full width at half maximum versus filenumber (bottom) Inverse of center of peak versus filenumber

In Fig. 4(top), the height of the peak verus file number is plotted and is in agreement with Fig. 1(left). The correlation length is related to the inverse of the width. In Fig. 4(bottom), the inverse of the peak center is plotted versus file number; the spacing of the magnetic domains is inverse to the peak center. In all cases the curves follow Fig. 1(left) more or less; the last one doesn't follow the second peak very well.

5. Conclusions

It is possible to see azimuthal intensity variation through data anaylsis of CCD images. Because of the odd behavior of the second peak and the differences in the autocorrelation functions(reflecting differences in electronic configurations) of the

first and second peaks, there appears to be a difference in the nature of the first and second peaks.

References

1. T. O. Mentes, C. Sanchez-Hanke and C. C. Kao, *J. Sync. Rad.* **9**, 90 (2002).
2. F. Yakhou, A. Letoublon, F. Livet, M. de Boissieu and F. Bley, *J. Magn. Magn. Mater* **233**, 119 (2001).
3. A. Rahmim, M.Sc. Thesis, Univ. of British Columbia, Vancouver, 2001.
4. N. E. Hunt, *Phase Retrieval and Zero Crossings: Mathematical Methods in Image Reconstruction* (Kluwer, Dordrecht, 1989).
5. A. Rahmim, S. Tixier, T. Tiedje, S. Eisebitt, M. Lorgen, R. Scherer, W. Eberhardt, J. Luning and A. Scholl, *Phys. Rev.* **B65**, 235421 (2002).
6. J. Benesty, D. R. Morgan and J. H. Cho, *IEEE Transactions on Speech and Audio Processing* **8**, 168 (2000).
7. M. Blume, in *Resonant Anomalous X-ray Scattering*, ed. G. Materlik *et al.* (Elsevier Science, Amsterdam, 1994), p. 495.
8. R. C. O'Handley, *Modern Magnetic Materials* (Wiley, New York, 2000).
9. D. H. Templeton, *Acta Cryst.* **A54**, 158 (1998).
10. S. Di Matteo, Y. Joly, A. Bombardi, L. Paolasini, F. de Bergevin and C. R. Natoli, *Phys. Rev. Lett.* **91**, 257402-1, (2003).